Int. J. Electrochem. Sci., 14 **(2019)** 6454 – 6467, doi: 10.20964/2019.07.67

International Journal of ELECTROCHEMICAL SCIENCE
www.electrochemsci.org

Graphene/Tungsten trioxide (Gr/WO_3) composite modified screen-printed carbon electrode for the sensitive electrochemical detection of nitrofurantoin in biological samples

S. Vetri Selvi[1], Ramachandran Rajakumaran[1], Shen-Ming Chen[1,], Ahmed Mostafa Rady[2], Selvakumar Veerasankar[3], Tse-Wei Chen[1,4], Syang-Peng Rwei[4,5], Bih-Show Lou[6,7*]*

[1] Electroanalysis and Bioelectrochemistry Lab, Department of Chemical Engineering and Biotechnology, National Taipei University of Technology, No. 1, Section 3, Chung-Hsiao East Road, Taipei 106, Taiwan.
[2] Zoology department, College of Science, King Saud University, P.O. Box 2455, Riyadh 11451, Saudi Arabia
[3] Integrated Technology Complex Department of Energy and Refrigeration Air-conditioning Engineering, National Taipei University of Technology, Taipei 10608, Taiwan
[4] Research and Development Center for Smart Textile Technology, National Taipei University of Technology, Taipei 106, Taiwan, ROC
[5] Institute of Organic and Polymeric Materials, National Taipei University of Technology, Taipei 106, Taiwan, ROC
[6] Chemistry Division, Center for General Education, Chang Gung University, Taoyuan, Taiwan,
[7] Department of Nuclear Medicine and Molecular Imaging Center, Chang Gung Memorial Hospital, Taoyuan, Taiwan
[*]E-mail: smchen78@ms15.hinet.net, blou@mail.cgu.edu.tw

Received: 6 April 2019 / *Accepted:* 19 May 2019 / *Published:* 10 June 2019

Graphene /tungsten trioxide (Gr/WO_3) composites were prepared by a simple method. This composite has been used as a potential electrode material for the electrochemical detection of nitrofurantoin (NTF). The as-prepared Gr/WO_3 composite was confirmed by X-ray diffraction (XRD), Field-emission scanning electron microscopy (FESEM), and Raman spectroscopy. Besides, the electrochemical properties of the prepared electrode were identified by different voltammetry techniques such as cyclic voltammetry (CV) and linear sweep voltammetry (LSV). The Gr/WO_3 composite modified screen printed carbon electrode (SPCE) shows an excellent electrocatalytic activity towards the detection of NTF. The Gr/WO_3/SPCE electrode detects NTF with a lower detection limit (0.002 µM), well linear response range (0.01 - 234 µM) and acceptable sensitivity (2.18 $\mu A \mu M^{-1} cm^{-2}$). Moreover, the Gr/WO_3 modified electrode exhibited good selectivity, reproducibility and higher stability when compared to other modified and unmodified electrodes. In addition to that, Gr/WO_3/SPCE modified electrode achieved appreciable recoveries for the determination of NTF in biological samples.

Keywords: Graphene, Tungsten trioxide, Electrochemical sensor**,** Nitrofurantoin, Real sample analysis.

1. INTRODUCTION

Nitrofurantoin (NTF) is a renowned antibiotic drug, belongs to the nitrofuran family and it has predominant antibacterial activity against gram positive and negative bacteria [1]. Especially it plays a vital role against bacteriophages such as *E.coli*, and *Salmonella enterica* [2, 3]. Generally, antibiotics are used to retard the growth of bacteria in humans and also to promote the feedstock efficiency among animal husbandry [4], and long-term prevention of bacterial infection in aquaculture [5]. Owing to the medical application, NTF is an organic synthetic derivative used for prophylaxis medication and also used for the treatment of urinary tract infection [6]. While, the overdosage of NTF causes mutagenicity, hepatotoxicity [7-9] and carcinogenic activity [10], besides that, prolonged usage of NTF leads to lung injury which results in pulmonary toxicity and other adverse side effects in humans including nausea, vomiting, diarrhea and peripheral neuropathy [11-12]. Oral intake of NTF is being unstable and quickly metabolize its function in the human body. Therefore, the usage of NTF was banned in many countries such as the United States, China, Thailand, European Union and Japan [13-14]. In order to overcome such issues, it is necessary to monitor and to develop the selective and sensitive method to detect dosage level of NTF. Until now, various analytical methods and techniques have been developed namely high-performance liquid chromatography, immunoassay, electrolysis, photoluminescence and polarography [15-23]. However, these techniques require more skilled persons to operate, pre-treatment of the sample and high cost. Nevertheless, electrochemical techniques have been equipped, because it provides numerous advantages such as low cost, portable, prompt response, high sensitivity, good stability and simplicity [24-28].

Among the other transition metal oxide nanocomposites such as NiO, TiO_2, SnO_2, ZnO, MoO_3 [29] and WO_3 are irresistible n-type semiconductors of wider band gap energy (2.4-2.8 eV) with extraordinary properties such as non-toxic, low-cost, chemically inert, highly stable in acidic environment and highly protective against photo corrosion, which leads to the increasing electrochemical activity towards sensing applications [30-31]. Due to its exceptional property, it has wide applications in various research fields such as photo catalyst [32], solar cells [33], photo degradation [34]. It is one of the prominent sensing materials towards hazardous pollutants, toxic and combustible gases [35-36]. Therefore, its electrochemical activity is improved by incorporating with carbon material like graphene, graphene oxide, carbon nanotube, and fullerene. Among them, graphene acquires unique arrangement of two-dimensional crystal lattice which is composed of hexagonal honeycomb structure with specified morphological property [37-38]. It has many attractive and fascinating properties in modifying electrodes for the electrochemical sensor applications due to its highly active surface area, excellent thermochemical stability, good electrical conductivity [39-41]. It has been used for various tremendous electrochemical application including lithium ion batteries, supercapacitor, and fuel cells [42-47]. More evidently, the implementation of Gr/WO_3 nanocomposite has been employed for the fabrication of electrochemical sensor towards NTF has never been reported

in the previous literature. Based on the following aspects, we believed that the combination of Gr and WO_3 is more susceptible for the electrochemical sensing of NTF.

Herein, we have developed Gr/WO_3 composite via simple wet-chemical method. As-prepared Gr/WO_3 composite were characterized by various analytical techniques. In addition to that, as synthesized Gr/WO_3 composite was used for the electrochemical sensing of NTF, which exhibits lower detection limit and high sensitivity.

2. EXPERIMENTAL SECTION

2.1 Materials and methods

Sodium tungstate dihydrate ($Na_2WO_4.2H_2O$), concentrated nitric acid (HNO_3), and commercial graphene was purchased from Sigma-Aldrich and used as received without further purification. The screen-printed carbon electrode (SPCE) was purchased from Zensor R&D Co., Ltd, Taiwan. The phosphate buffer solution (0.05 M PBS) for the preparation of electrolyte solutions was prepared by mixing of monosodium phosphate (NaH_2PO_4) and disodium phosphate (Na_2HPO_4). The required solutions and reagents were prepared using Millipore water system.

The surface morphology of graphene, as-prepared WO_3 and Gr/WO_3 nanocomposite were investigated by powder X-ray diffraction analysis (XRD, D/MAX-IIIA diffractometer (λ = 0.15406 nm). The Raman spectroscopy studies was analyzed by using NT-MDT, NTEGRA SPECTRA instrument. Scanning electron microscope (SEM) and EDX spectral studies were carried by using Hitachi S-3000H (SEM Tech Solutions, USA) and HORIBA EMAX X-ACT, respectively. All the electrochemical experiments were carried out at room temperature by CV and LSV techniques using CHI 1205C and CHI 900 electrochemical workstation containing conventional three electrode cell system composed of SPCE as a working electrode (working surface area of about 0.035 cm^2), platinum wire used as an auxiliary electrode and Ag/AgCl (sat. KCl) as reference electrode.

2.2 Synthesis and fabrication of WO_3 Nanosheets and Gr/WO_3 composite

The synthesis procedure of nanoflakes like WO_3 was followed by previously reported article with sight modification [62]. In briefly, 1g of $Na_2WO_4 \cdot 2H_2O$ was dissolved in 200 mL of concentrated HNO_3 (4.8 M) under vigorous stirring for 1 h. The resultant yellow precipitate was centrifuged and washed with water until attaining neutral pH, followed by ethanol and dried at 80 °C for overnight. Finally, the obtained products were calcined at 500 °C for 3 h. The as-prepared WO_3 nanoflakes were taken for the further electrochemical applications. For the composite preparation and fabrication process, 0.003 g of graphene was dissolved into the solvent containing 1 mL ethanol and sonicated for 20 mins. Then, 0.002 g of as-prepared WO_3 nanoflakes were added to the above solution and kept for 30 min in ultrasonication path to get homogeneous suspension. Later, the SPCE surface was washed with water and ethanol to remove the impurities on the electrode surface. Then, about 6 µL of above suspension was drop coated on the electrode and dried at ambient temperature in oven. The dried nanocomposite modified electrode was gently washed with water to remove the loosely attached

molecules on the SPCE surface. The dried modified electrode designated as Gr/WO_3/SPCE and directly used for further electrochemical experiments. The overall synthesis route of Gr/WO_3 composite and the electrochemical applications is shown in Scheme 1.

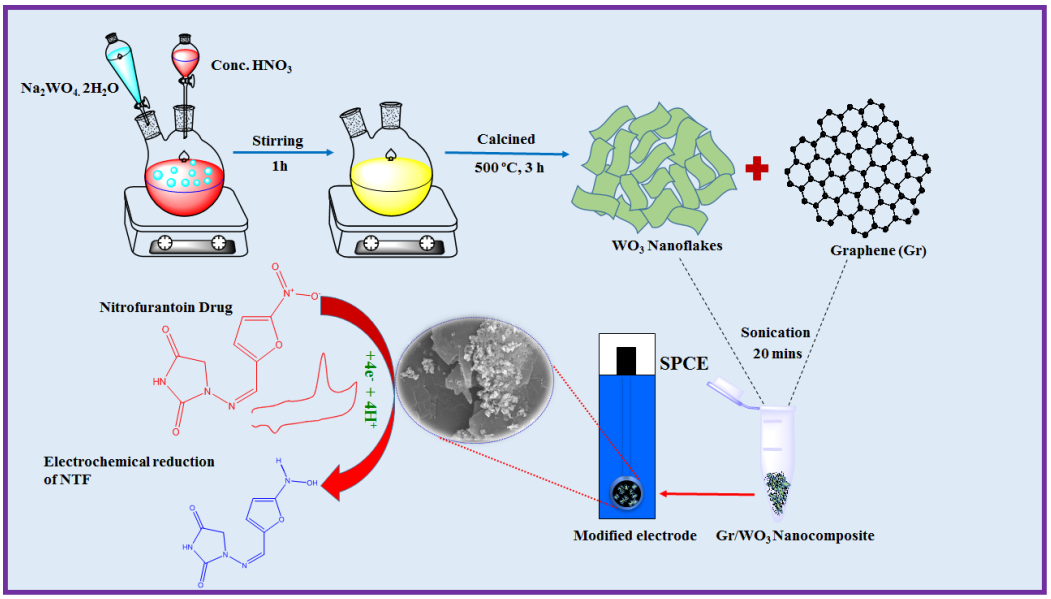

Scheme 1. Synthesis procedure of Gr/WO_3 composite and the electrochemical detection of NTF.

3. RESULTS AND DISCUSSION

3.1 Structural and surface morphological investigation

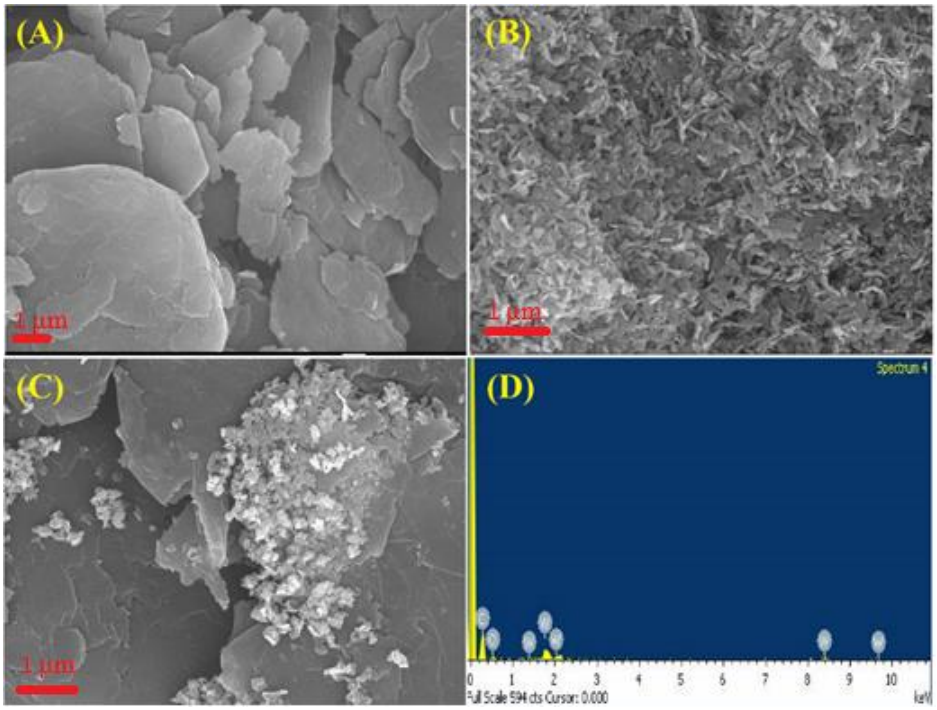

Figure 1. (A) FE-SEM images of graphene, (B) WO_3, (C) Gr/WO_3 nanocomposite and (D) EDX spectrum of Gr/WO_3 composite.

The surface morphology of graphene, WO_3 and Gr/WO_3 nanocomposite were investigated by FE-SEM analysis. Fig. 1A, represents nanosheet like structured graphene. Graphene layer is composed of multilayer arrangement of carbon sheets. On the other hand, as-prepared WO_3 are exist in the form of uniformly sized nanoflakes with <100 nm range as shown in Fig. 1B. Fig. 1C shows that the WO_3 nanoflakes anchored on the layers of Gr and it clearly confirmed the formation of Gr/WO_3 composite. In order to examine the elemental composition of Gr/WO_3 composite, EDX analysis were scrutinized and shown in Fig. 1D. From EDX analysis, it is confirmed that the presence of W, C, and O elements in an appropriate ratio. The absence of any other elemental or impurity peaks confirming the purity of the nanocomposite synthesized. At finally, it is established that the Gr/WO_3 composite were successfully formed with even size and smooth surface morphology.

3.2 Crystallinity and phase purity studies

Further, XRD analysis of graphene, WO_3 and Gr/WO_3 composite were exposed in Fig. 2(A-C). Diffraction pattern of Gr was shown in Fig. 2A. The sharp intense peak at It gives evidence for the existence of several lattice planes such as (002), and (100). In addition to that, XRD pattern of WO_3 Fig. 2B consist of some diffraction planes such as (100), (200), (130), (202), (122), and (004). Similarly, XRD patterns of Gr/WO_3 nanocomposite exhibits several lattice planes such as (100), (200), (120), (122), (022), (222), (004), (140), and (420) which is corresponding to the cubic crystal lattice of isometric phase of WO_3 nanoflakes (JCPDS No. 20-1324) and shown in Fig. 2C [48- 50]. All the above results proved that the successful formation of Gr/WO_3 nanocomposite by wet-chemical and sonochemical method without any other impurities.

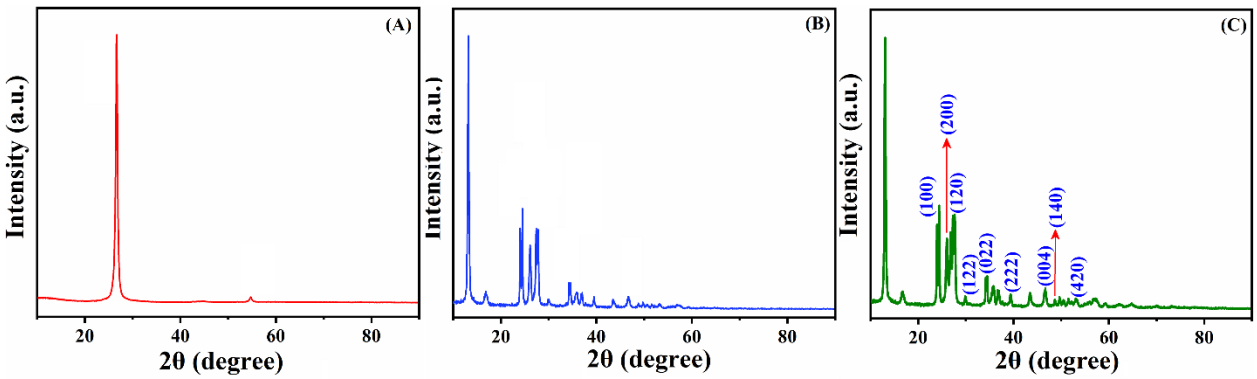

Figure 2. (A), XRD pattern of graphene (B), WO_3 and (C) Gr/WO_3 composite.

3.3 Raman spectral analysis

Raman spectra of graphene, WO_3 and Gr/WO_3 nanocomposite were shown in Fig. 3(A-C). From Fig. 3(A-C), sharp band of G, broad D, G, and 2D bands were observed and presence of some disorder which could be formed due to surface phenomena. A sharp band at 200 cm^{-1} can be ascribed to the lattice vibrations of WO_3. The bands at 327 and 524 cm^{-1} ascribed to the (O-W-O) deformation vibrations and the band at 712 and 804 cm^{-1} are assigned for (O-W-O) stretching vibrations. These

results clearly point out the formation of monoclinic tungstic oxide and well matches with XRD data. At the same time, incorporation of Gr leads to the decrease in crystallinity of WO_3, which is visible in lowered intensities and broadening of bands corresponding to the monoclinic WO_3. These results confirmed the complete incorporation of WO_3 on the graphene sheets. Additionally, band crystallinity confirmation WO_3 corresponds to the lattice vibrations at 251.4 cm^{-1} represents (O-W-O) the deformation, and vibrations modes at 524, 712, 817.2 cm^{-1} corresponds to the (O-W-O) stretching vibrations. At finally, Raman analysis proved that the defective sites were present in the Gr/WO_3 nanocomposite and this property enhances the electrochemical activity [51-55].

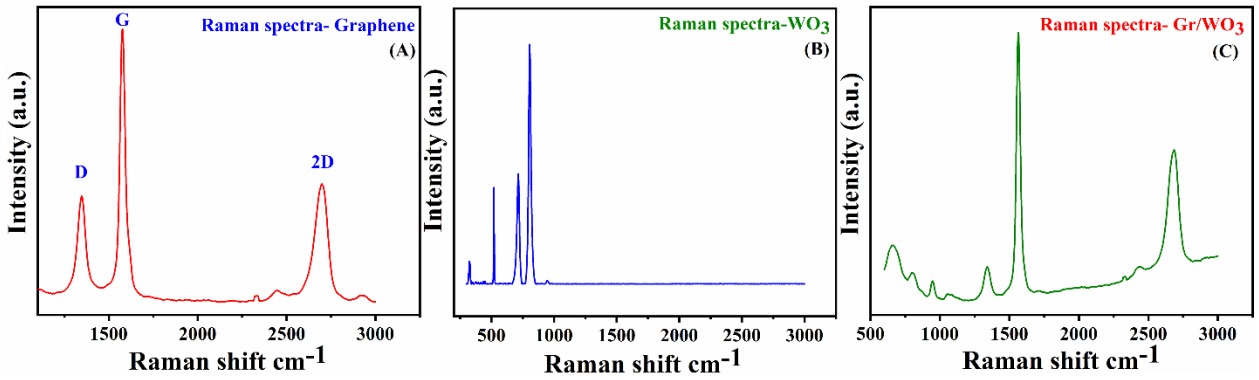

Figure 3. (A) Raman spectra of Gr, (B) WO_3 and (C) Gr/WO_3 composite.

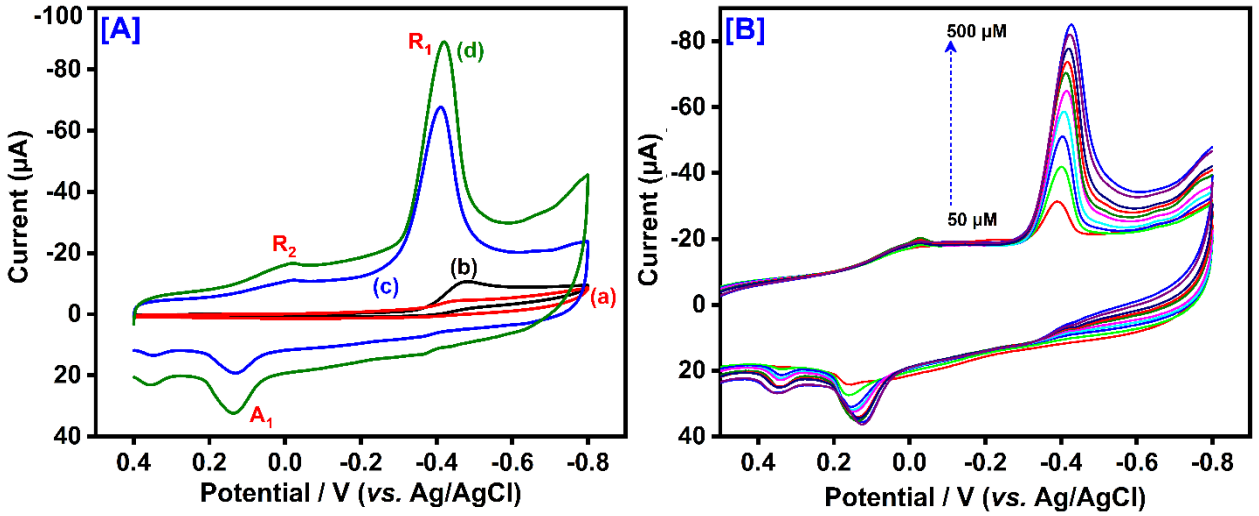

Figure 4. (A) CVs of 500 µM NTF in 0.05 M PBS (pH 7.0) at the bare SPCE (a), WO_3/SPCE (b), Gr/SPCE (c) and Gr/WO_3/SPCE (d). (B) Various concentration of NTF at Gr/WO_3/SPCE from 50 to 500 µM. Scan rate: 50 mV/s. Potential window: 0.4 to -0.8 V.

3.3 Electrocatalytic detection of NTF at different modified electrodes

The electrochemical behavior of the Gr/WO_3/SPCE electrode towards the detection of NTF was identified by CV and LSV techniques. Furthermore, the electrocatalytic activity at Gr/WO_3/SPCE

for the detection of NTF was compared with other modified electrodes. Fig. 4A exhibits the typical CV response curves of (a) bare SPCE, (b) WO_3/SPCE, (c) Gr/SPCE and (d) Gr/WO_3/SPCE in the presence of 500 µM NTF in N_2 saturated pH 7.0 nature of 0.05 M PBS solution at a scan rate of 50 mV/s with the potential range of 0.4 to -0.8 V. The bare SPCE exhibit the small cathodic peak at -0.47 V with current density of 4.4 µA. The Gr/SPCE electrode shows the higher cathodic peak of NTF at -0.41 V with peak current perfromance of 68 µA. The WO_3/SPCE electrode shows a notable cathodic peak performance at -0.46 V with current density response of 10.9 µA. The Gr/WO_3/SPCE electrode exhibited a higher cathodic peak R_1 current density of 89.3 µA at the peak potential of -0.41 V. Therefore, NTF detection perfromance was highly facilitated at the Gr/WO_3/SPCE electrode displays excellent current response towards the detection of NTF due to the high conducting properties and excellent electrocatalytic properties. The obtained R_1 peak is associated to the direct reduction (irreversible) of NTF to hydroxylamine group with four electron and proton transfer process. Further, one more redox peak was observed and it was denoted as R_2/A_1. The reversible peak is related to the redox behavior between hydroxylamine to nitroso derivatives with two electron and two proton process. The obtained electrochemical peaks and their corresponding reduction and redox mechanisms were clearly explained and well documented in the previous literature [56]. The overall reduction and redox electrochemical mechanism of NTF is depicted in Scheme 2. The enhanced electrocatalytic activity and low peak potential were attributed to the synergistic effect of Gr and WO_3 nanoflakes. It was found that, the Gr/WO_3/SPCE sensor electrode had the look of best performance towards the determination of NTF.

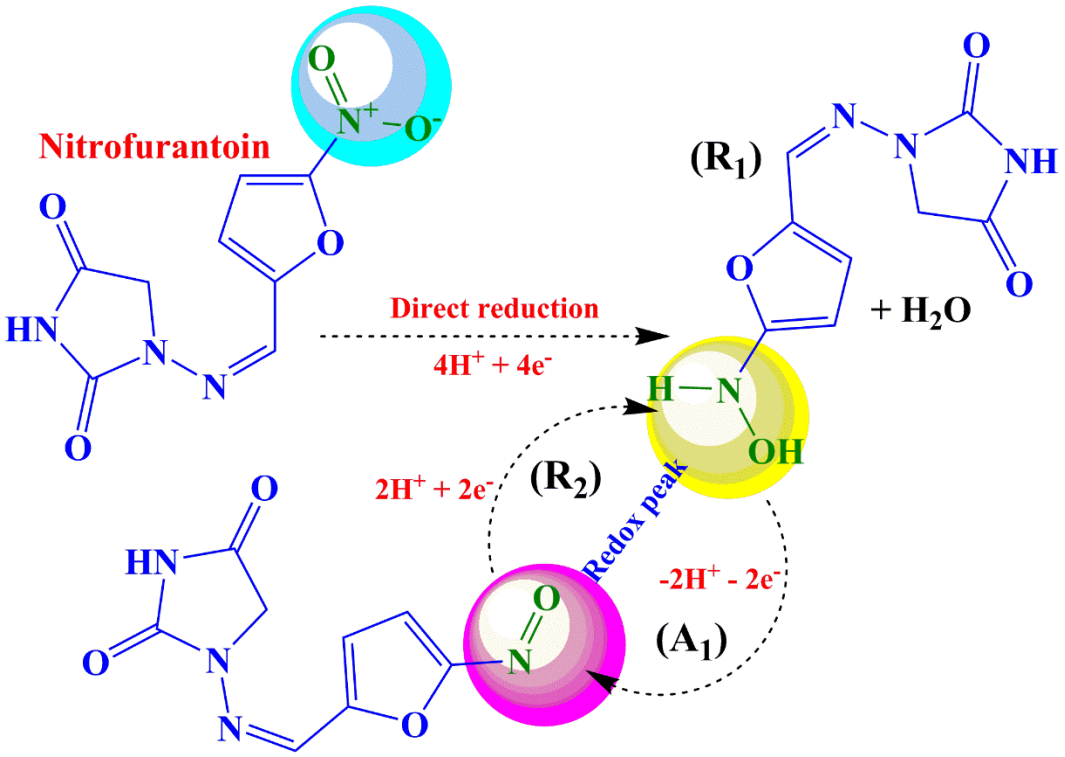

Scheme 2. The overall electrochemical reduction and redox mechanism of NTF at Gr/WO_3/SPCE

3.4 Influence of concentration

The electrocatalytic behavior of the Gr/WO_3/SPCE electrode towards the determination of different concentrations of NTF was identified by CV containing 0.05 M PBS (pH 7.0) at a scan rate of 50 mV/s (Fig. 4B). Increasing the different concentration of NTF from 50 to 500 µM, the reduction peak current was increased by the reduction of NTF on the Gr/WO_3/SPCE electrode surface. The electrochemical features such as correlation co-efficient, sensitivity, linear response range and limit of detection of NTF at the modified electrode has been briefly discussed in the determination section (see section 3.7).

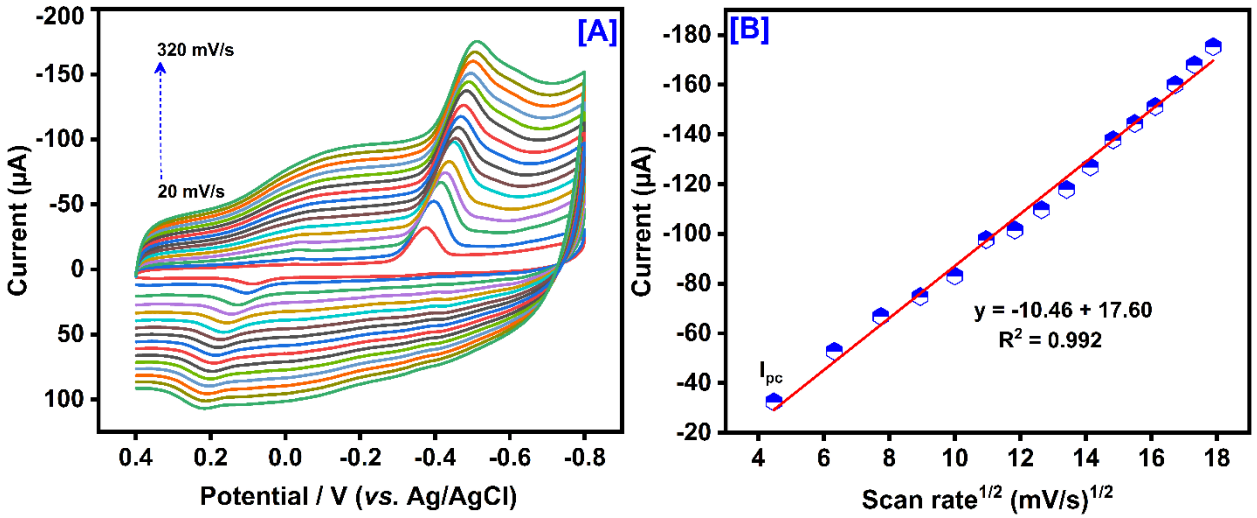

Figure 5. (A) CVs for Gr/WO_3/SPCE in 0.05 M PBS (pH 7.0) containing 500 µM of NTF at different scan rate from 20 to 320 mV/s. (B) The linear relationship between the cathodic peak current *vs.* square root of scan rate.

3.5 Influence of scan rate

The electrode reaction of the modified electrode towards detection of NTF was strongly influenced by the scan rate as shows in Fig. 5A. The CV performance of the Gr/WO_3/SPCE electrode in 0.05 M PB solution (pH 7.0) with 500 µM NTF was investigated at different scan rates ranging from 20-320 mV/s. It can be clearly shows the cathodic peak current of NTF at the Gr/WO_3/SPCE electrode was increased linearly with increasing the scan rate and the reduction peak potential was slightly shifted towards more negative potential. Fig. 5B exhibit the linear relationship between the peak current and the square root of scan rate (20 - 320 mV/s) with a linear regression equation of I_{pc} (µA) = -10.46 + 17.60 (R^2 = 0.992). These results clearly suggest that the electrochemical detection of NTF at the Gr/WO_3/SPCE electrode was a diffusion-controlled electrochemical reaction.

3.6 Influence of pH

An influence of pH on the electrochemical detection performance of 500 µM NTF at the Gr/WO_3/SPCE electrode, identified by CV in the pH range of 3.0 - 11.0 at a scan rate of 50 mV/s and the obtained CV curves displayed in Fig. 6A. The reduction peaks current was increased with increasing the pH value up to pH 7.0 and then gradually decreased. The peak potential (E_{pc}) of the electrode shifted towards positive and negative direction while adjusting the pH values from lower and higher, which indicating that the electrochemical behavior of NTF is pH dependent electrochemical reaction. Moreover, Fig. 6B exhibit the calibration plot between the pH and reduction peak current. The pH studies show the maximum reduction peak current was obtained at pH 7.0. Hence, the pH 7.0 was selected as the optimum pH value for the electrochemical determination of NTF.

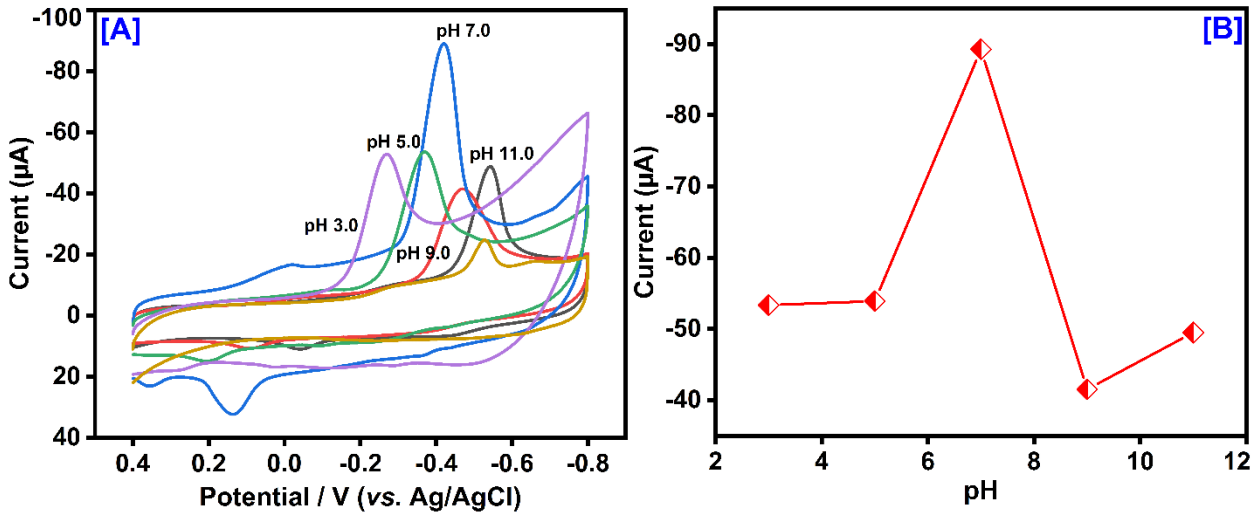

Figure 6 (A) CVs of Gr/WO_3/SPCE at various pH values (pH 3.0 – 11.0) vs. scan rate at 50 mV/s, (B) The calibration plot for the pH *vs.* cathodic peak current (R_1).

3.7 Determination of NTF at Gr/WO_3 modified SPCE

Due to the more quantitative characteristic of linear sweep voltammetry (LSV) compared to CV technique, LSV analysis was utilized to obtain the analytical figures. In order to get the calibration curve, the measurements were done in 0.05 M PBS (pH 7.0) with the NTF addition from the concentration of 0.1 – 1614 µM (Fig. 7A). The analytical peak current shows linearity in the NTF concentration ranges from 0.01 to 234 µM (Fig. 7B) with a lower detection limit (LOD) of 0.002 µM. The LOD was calculated by using the following equation (1),

$$LOD = 3s/b \quad (1)$$

where ‘s’ is the average standard deviation of three measurements for the blank solution and ‘b’ is the sensitivity calculated from the slope value of calibration plot (2.18 $\mu A \mu M^{-1} cm^{-2}$). The lower LOD of the Gr/WO_3/SPCE modified sensor may be attributed to the higher electrocatalytic activity, high surface area, and strong interaction between the electrode and NTF analyte in the electrolytic solution. The obtained analytical performances such as LOD, linear response range, sensitivity of the

Gr/WO_3/SPCE electrode was also compared with a previously reported NTF sensor, and the results are summarized in Table 1. The performance of the Gr/WO_3/SPCE was more efficient than that of the previously reported NTF sensor. Therefore, the Gr/WO_3/SPCE electrode is an excellent electrode material for the electrochemical detection and determination of NTF at the nanomolar level.

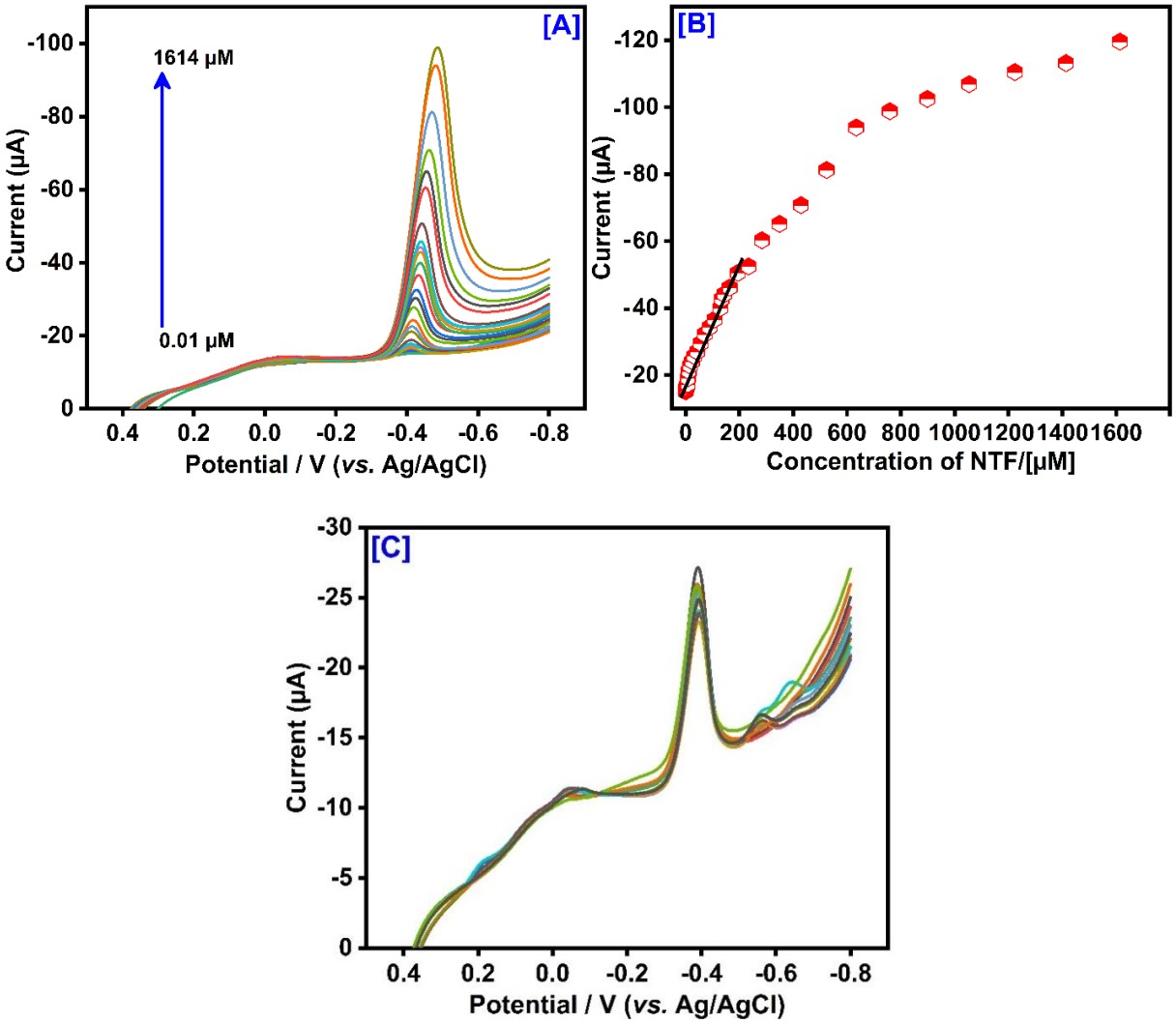

Figure 7. (A) LSVs of Gr/WO_3/SPCE at various concentration (0.01 – 1614 µM), scan rate at 50 mV/s, (B) The calibration plot for the concentration of NTF *vs.* cathodic peak current (R_1), (C) Interference studies at Gr/WO_3/SPCE with various interfering species.

3.8 Interference studies and real sample analysis

The selectivity of the Gr/WO_3/SPCE was studied by the NTF sensor response in the presence of other interfering compounds in 0.05 M PB solution (pH 7.0) and the current signal changes were examined by LSV techniques. Fig. 7C shows the LSV current response of NTF and other foreign species such as caffeic acid, chloramphenicol, catechol, dopamine, glucose, 4-nitrobenzene, uric acid, metronidazole, hydroquinone, $NaNO_2^-$, 4-nitrophenol, and KCl. However, the presence of aforementioned interfering compounds shows negligible peak current response compared to the NTF

detection signal with a deviation of less than 5%. These results clearly suggested that the Gr/WO_3/SPCE electrode displayed significant selectivity and well anti-interference ability towards NTF sensing.

Table 1. Analytical performances of different modified electrodes for NTF determination

Electrode	Linear range (µM)	LOD (µM)	Ref.
$Nd_2Mo_3O_9$	0.1–1331	16	[56]
Boron-doped diamond	0.497–5.66	27.2	[57]
DsDNA/PAMT/SPCE	8.4–105.0	2.73	[58]
Cetrimide	0.1–20	0.06 and 0.27 ng/mL	[59]
Cobalt/GCE	0.06–5	0.01	[60]
CNF/SPE	0.08 – 320	0.016	[61]
Au/AuNR	3.0-500	0.18	[63]
PME/MWCNT/SPCE	0.05-2.0	0.012	[64]
Gr/WO_3/SPCE	0.01-234	0.002	This work

The electrochemical activity of Gr/WO_3/SPCE is considered to be more important framework to detect NTF in real sample analysis such as biological and water samples. The LSV technique was used for practical analysis to detect NTF in human urine and water sample, as a standard addition tool was utilized for the recovery calculation. However, the prepared samples do not contain NTF, therefore, a known concentration of NTF was added into the real samples and these spiked samples were directly used for electrochemical investigations. The working condition, parameters and all other procedure followed by the LSV determination section 3.7. The chosen real samples and obtained results are summarized in Table 2. From the Table 2, the recovery values of about 98.4 to 99.7% in urine and water samples. The Gr/WO_3/SPCE electrode successfully reveals the detection of NTF in real samples with acceptable recovery and it acts as a potential electrode material for use in practical applications.

Table 2. Real sample analysis towards NTF detection

Samples	Added (µM)	Found (µM)	Recovery (%)
Human urine	5.0	4.92	98.4
	7.0	6.98	99.7
Tab water	5.0	4.97	99.4
	7.0	6.91	98.7

3.9 Repeatability and stability studies

The repeatability of the Gr/WO_3/SPCE electrode were identified by CV technique with concentration of 500 µM NTF. For the repeatability studies on the Gr/WO_3/SPCE electrode was confirmed with 10 consecutive measurements by a single modified electrode. Moreover, the RSD of the single Gr/WO_3/SPCE electrode was found to be 2.04% for NTF sensing. The storage stability of

the Gr/WO_3/SPCE electrode was investigated up to 7 days by the CV techniques. After 7 days the NTF current signal was observed with slight variation and loss only at 2.7% of the initial peak current response due to the excellent stability. These above results indicate that the Gr/WO_3/SPCE electrode has good stability and efficient repeatability towards the electrochemical sensing of NTF.

4. CONCLUSION

In summary, Gr/WO_3/SPCE have been prepared successfully through a simple wet-chemical approach and followed by sonochemical technique and further applied to the electrochemical detection of NTF. The structure of the Gr/WO_3 was characterized by various physical and chemical characterization techniques. The electrocatalytic behavior of the Gr/WO_3/SPCE were identified by CV and LSV techniques. The Gr/WO_3/SPCE modified electrode delivers high electrocatalytic activity towards the detection of NTF, low detection limit (0.002 μM), with a broader linear response range (0.01 - 234 μM) and excellent sensitivity (2.18 $\mu A \mu M^{-1} cm^{-2}$). Besides, the Gr/WO_3/SPCE electrode have excellent repeatability, selectivity, stability, and practical feasibility. These results indicate that the Gr/WO_3/SPCE electrode can be used as an eminent and advanced electrode materials for the sensitive detection of NTF.

ACKNOWLEDGEMENT
The authors gratefully acknowledge the financial support of the Ministry of Science and Technology, Taiwan through contract nos. MOST 107-2221-E-182-021 and MOST 107-2113-M-027-005-MY3. The financial support from the Chang Gung Memorial Hospital through contract no. CMRPD5H0031 to B.S. Lou is also acknowledged. Also, this project was supported by King Saud University, Deanship of Scientific Research, College of Science, Research Center.

References

1. L.S. Goodman, A.G. Gilman, T.W. Rall and F. Murad, *Pharmacol. Basis Ther*., (1985) 446.
2. T. Shoda, K. Yasuhara, M. Moriyasu, T. Takahashi and C. Uneyama, *Arch. Toxicol*., 75 (2001) 297.
3. M. Khodari, H. Mansour and Gaber A.M. Mersal, *J. Pharm. Biomed. Anal.*, 20 (1999) 579.
4. M.S.U. Rehman, N. Rashid, M. Ashfaq, A. Saif, N. Ahmad and J.I. Han, *Chemosphere*., 138 (2015) 1045.
5. I. Kaniou, G. Zachariadis, G. Kalligas, H. Tsoukali and J. Stratis, *J. Liq. Chromatogr*., 17 (1994) 1385.
6. P. Muth, R. Metz, B. Siems, W.W. Bolten and H. Vergin, *J. Chromatogr. A*., 729 (1996) 251.
7. S.S. Jick, H. Jick, A.M. Walker and J.R. Hunter, *Chest*., 96 (1989) 512.
8. G. Amit, P. Cohen and Z. Ackerman, *Isr. Med. Assoc. J.* 4 (2002) 184.
9. I.L. Tan, M.J. Polydefkis, G.J. Ebenezer, P. Hauer and J.C. McArthur, *Arch. Neurol*. 69 (2012) 265.
10. D.R. McCalla, *Environ. Mutagen*., 5 (1983) 745.
11. Clinical and research information on drug-induced liver injury, https://livertox.nlm.nih.gov/Nitrofurantoin.htm (2019)
12. B.A. Cunha, *Obstet. Gynecol. Surv*. 44 (1989) 399.

13. L.A.P. Hoogenboom, M.V.A.N. Kammen, M.C.J. Berghmans, J.H. Koeman and H.A. Kuiper, *Food Chem. Toxicol*. 29 (1991) 321.
14. FAO: Nitrofuran study Archived 2008-12-04 at the Wayback Machine.
15. W. P. Sutthivaiyakit and S. Sutthivaiyakit, *Anal. Lett*., 48 (2015) 1979.
16. W. H. Yu, T. S. Chin and H. T. Lai, *Int. Biodeterior. Biodegrad*., 85 (2013) 517.
17. W. Liu, C. Zhao, Y. Zhang, S. Lu, J. Liu and R. Xi, *J. Agric. Food Chem*., 55 (2007) 6829.
18. Q. Wang, Y. C. Liu, Y. J. Chen, W. Jiang, J. L. Shi, Y. Xiao and M. Zhang, *Anal. Methods*, 6 (2014) 4414.
19. L. Q. Sheng, M. M. Chen, S. S. Chen, N. N. Du, Z. D. Liu, C. F. Song and R. Qiao, *Food Addit. Contam., Part A*, 30 (2013) 2114.
20. N. N. Du, M. M. Chen, L. Q. Sheng, S. S. Chen, H. J. Xu, Z. D. Liu, C. F. Song and R. Qiao, *J. Chromatogr. A*, 1327 (2014) 90.
21. Y. Wang, T. Chen, Q. Zhuang and Y. Ni, *Talanta*, 179 (2018) 409.
22. G.G. Parra, L.P. Ferreira, D.C.K. Codognato, C.C.S. Cavalheiro and I. Borissevitch, *J. Lumin*., 185 (2017) 10.
23. Y. Wang, T. Chen, Q. Zhuang, and Y. Ni, *Talanta.*, 179 (2018) 409.
24. P. Balasubramanian, R. Settu, S.M. Chen, T.W. Chen, and G. Sharmila, *J. Colloid Interface Sci*., 524 (2018) 417.
25. H. Karimi-Maleh, P. Biparva, and M. Hatami, *Biosens. Bioelectron*., 48 (2013) 270.
26. R. Karthik, Y.S. Hou, S.M. Chen, A. Elangovan, M. Ganesan, and P. Muthukrishnan, *J. Ind. Eng. Chem*., 37 (2016) 330.
27. J.V. Kumar, R. Karthik, S.M. Chen, V. Muthuraj, and K. Chelladurai, *Sci. Rep*., 6 (2016) 34149.
28. N. Karikalan, R. Karthik, S.M. Chen, M. Velmurugan, and C. Karuppiah, *J. Colloid. Interface Sci*., 483 (2016) 109.
29. M. Abinaya, K. Saravanakumar, E. Jeyabharathi and V. Muthuraj, J. Inorg. Org. Polymer. Mater., 29 (2019) 101.
30. J. Su, L. Guo, N. Bao, and C.A. Grimes, *Nano Lett*., 11 (2011) 1928.
31. S. Jing, H. Zheng, L. Zhao, L. Qu, and L. Yu, *Talanta*, 174 (2017) 477.
32. J. Su, X. Feng, J. D. Sloppy, L. Guo and C. A. Grimes, *Nano Lett*., 11 (2010) 203.
33. H. Zheng, Y. Tachibana, and K. Kalantar-zadeh, *Langmuir*, 26 (2010) 19148.
34. X. Su, Y. Li, J. Jian, and J. Wang, *Mater. Res. Bull*., 45 (2010) 1960.
35. M. Stankova, X. Vilanova, E. Llobet, J. Calderer, M. Vinaixa, and I. Gracia, *Thin Solid Films*., 500 (2006) 302.
36. T. Kida, A. Nishiyama, Z. Hua, K. Suematsu, M. Yuasa, and K. Shimanoe, *Langmuir*, 30 (2014) 2571.
37. D. Chen, H. Feng and J. Li, *Chem. Rev*., 112 (2012) 6027.
38. H. P. Cong, J. F. Chen and S. H. Yu, *Chem. Soc. Rev*., 43 (2014) 7295.
39. M.D. Stoller, S.J. Park, Y.W. Zhu, J.H. An, and R.S. Rouff, *Nano Lett*., 8 (2008) 3498.
40. A.A. Balandin, S. Ghosh, W.Z. Bao, I. Calizo, D. Teweldebrhan, F. Miao, and C.N. Lau, *Nano Lett.,* 8 (2008) 902.
41. S. Yang, X. Feng, S. Ivanovici, and K. Müllen, *Angew. Chem. Int. Ed*., 49 (2010) 8408.
42. I. I. Bobrinetskiy and N. Z. Knezevic, *Anal. Methods*, 10 (2018) 5061.
43. Y. H. Wang, Y. X. Chen, X. Wu and K. J. Huang, *Colloid. Surf. B*, 172 (2018) 407.
44. Y. H. Wang, K. J. Huang, X. Wu, Y. Y. Ma, D. L. Song, C. Y. Du and S. H. Chang, *J. Mater. Chem. B*, 6 (2018) 2134.
45. N. Atar, T. Eren, M.L. Yola, H. Gerengi, and S. Wang, *Ionics*, 21 (2015) 3185.
46. M.D. Stoller, S. Park, Y. Zhu, J. An, and R.S. Ruoff, *Nano Lett.,* 8 (2008) 3498.
47. O. Akyıldırım, H. Yüksek, H. Saral, I. Ermis, T. Eren, and M.L. Yola, *J. Mater. Sci. Mater. Electron*., 27 (2016) 8559.

48. N. H. Kim, S.J. Choi, S.J. Kim, H.J. Cho, J.S. Jang, W.T. Koo, M. Kim, and I.D. Kim, *Sens. Actuat., B* 224 (2016) 185.
49. A. Hoel, L. Reyes, S. Saukko, P. Heszler, V. Lantto, and C. Granqvist, *Sens. Actuat. B*, 105 (2005) 283.
50. Z. Zhang, X. Wang, Z. Cui, C. Liu, T. Lu, and W. Xing, *J. Power Sources*., 185 (2008) 941.
51. G. Jeevitha, R. Abhinayaa, D. Mangalaraj and N. Ponpandian, *J. Phys. Chem. Solid*., 116 (2018) 137.
52. Shubhda Srivastava, Kiran Jain, V N Singh, Sukhvir Singh, N Vijayan, Nita Dilawar, Govind Gupta and T D Senguttuvan, *Nanotech*., 23 (2012) 205501
53. Xiaoxiao Hu, Peiquan Xu, Hongying Gong and Guotao Yin, *Mater.*, 11 (2018) 147.
54. Haoyu Wu, Ming Xu, Peimei Da, Wenjie Li, Dingsi Jia and Gengfeng Zheng, *Phys.Chem. Chem. Phys*., 15 (2013) 16138
55. Yufeng Hao, Yingying Wang, Lei Wang, Zhenhua Ni, Ziqian Wang, Rui Wang, Chee Keong Koo, Zexiang Shen, and John T. L. Thong, *Small*, 6 (2010) 195
56. J.V. Kumar, R. Karthik, S.M. Chen, K.H. Chen, S. Sakthinathan, V. Muthuraj, and T.W. Chiu, *Chem. Eng. J*., 346 (2018) 11.
57. P. de Lima-Neto, A.N. Correia, R.R. Portela, M. da Silva Julião, G.F. Linhares-Junior, and J.E. de Lima, *Talanta*., 80 (2010) 1730.
58. G. Aydo˘gdu, G. G¨unendi, D. K. Zeybek, B. Zeybek and S¸. Pekyardımc, *Sens. Actuat. B*, 197 (2014) 211.
59. R. Jain, A. Dwivedi, and R. Mishra, *J. Hazard. Mater*., 169 (2009) 667.
60. X.C. Tan, J.D. Qiu, Y. Li, X.Y. Zou, and P.X. Cai, *Chin. J. Anal. Chem*., 32 (2004) 930.
61. P. Salgado-Figueroa, P. Jara-Ulloa, A. Alvarez-Lueje, and J.A. Squella, *Electroanalysis*, 25 (2013) 1433.
62. D. Xue, J.Wang, Y.Wang, G.Sun, J.Cao, Hari Bala, and Z.Zang, *Nanomaterials*, 9(3) 2019 351.
63. A. Rahi, N. SAttarahmady, R. Dehdari Vais, and H.Heli, *Sens. Actuat. B.*, 210 (2015) 96.
64. S.H.Chiu, Y.L.Su, Anh V. T. Le, and S.H.Cheng , *Analy and Bioanal*., 410 (2018) 6573.